HHS Public Access

Author manuscript

Lab Invest. Author manuscript; available in PMC 2016 November 30.

Published in final edited form as:

Lab Invest. 2016 August ; 96(8): 895–908. doi:10.1038/labinvest.2016.61.

C/EBP homologous protein modulates liraglutide-mediated attenuation of non-alcoholic steatohepatitis

Khalidur Rahman[#§,1,3], **Yunshan Liu**[#3], **Pradeep Kumar**[1], **Tekla Smith**[1,3], **Natalie E. Thorn**[1], **Alton B. Farris**[2], and **Frank A. Anania**[1,3]

[1]Division of Digestive Diseases, Emory University, Atlanta, GA

[2]Department of Pathology, Emory University Hospital, Atlanta, GA

[3]Atlanta VA Medical Center, Decatur, GA

[#] These authors contributed equally to this work.

Abstract

The CCAAT/enhancer-binding protein (C/EBP) homologous protein (CHOP), a major transcriptional regulator of endoplasmic reticulum (ER) stress-mediated apoptosis, is implicated in lipotoxicity-induced ER stress and hepatocyte apoptosis in non-alcoholic fatty liver disease (NAFLD). We have previously demonstrated that the glucagon like peptide 1 (GLP-1) agonist, liraglutide, protects steatotic hepatocytes from lipotoxicity-induced apoptosis by improved handling of free fatty acid (FFA)-induced ER stress. In the present study, we investigated whether CHOP is critical for GLP-1 mediated restoration of ER homeostasis and mitigation of hepatocyte apoptosis in a murine model of NASH (non-alcoholic steatohepatitis). Our data show that despite similar caloric intake, CHOP KO (*CHOP*$^{-/-}$) mice fed a diet high in fat, fructose, and cholesterol (HFCD) for sixteen weeks developed more severe histological features of NASH compared with wild type (WT) controls. Severity of NASH in HFCD-fed *CHOP*$^{-/-}$ mice correlated with significant decrease in peroxisomal β-oxidation, and increased *de novo* lipogenesis and ER stress-mediated hepatocyte apoptosis. Four weeks of liraglutide treatment markedly attenuated steatohepatitis in HFCD-fed WT mice by improving insulin sensitivity, and suppressing *de novo* lipogenesis and ER stress-mediated hepatocyte apoptosis. However, in the absence of CHOP, liraglutide did not improve insulin sensitivity, nor suppress peroxisomal β-oxidation or ER stress-mediated hepatocyte apoptosis. Taken together, these data indicate that CHOP protects hepatocytes from HFCD-induced ER stress, and plays a significant role in the mechanism of liraglutide-mediated protection against NASH pathogenesis.

Keywords

non-alcoholic fatty liver disease; non-alcoholic steatohepatitis; C/EBP homologous protein; apoptosis

[§]Corresponding Author: Khalidur Rahman, PhD, Assistant Professor of Medicine, Emory University School of Medicine, 615 Michael Street, Suite 201, Atlanta, GA 30322, Phone: 404-712-2867 or 404-727-5638, Fax: 404-727-5767 reben.rahman@emory.edu.

Conflict of interest: All authors declare no conflicting interests.

Non-alcoholic fatty liver disease (NAFLD) represents a broad spectrum of disorders including benign non-alcoholic fatty liver-or bland steatosis (NAFL), to the more severe non-alcoholic steatohepatitis (NASH) and steatofibrosis[1, 2]. According to recent reports, the prevalence of NAFL ranges from 20-30% in the general population and as high as 75-100% in obese individuals[3, 4]. Although most NAFL patients remain asymptomatic, one fifth of NAFL patients progress to chronic hepatitis (NASH), which can further progress to cirrhosis, portal hypertension, and promote development of hepatocellular carcinoma (HCC)[4, 5]. Despite its high prevalence, and established morbidity and mortality associated with NAFLD, mechanisms leading to NAFLD progression remain poorly understood.

Systemic insulin resistance, lipotoxicity, and oxidative stress are central players in the pathogenesis of NASH[6-8]. Recent studies indicate that the unfolded protein response (UPR), an adaptive response that regulates ER function during ER stress through transcriptional and translational modulation of factors involved in ER homeostasis, also plays a critical role in free fatty acid (FFA) and free cholesterol mediated lipotoxicity[8-14]. Under conditions of nutrient overload, excess FFA and cholesterol induce activation of the UPR[9, 14]. Failure of the UPR to maintain ER homeostasis in the setting of metabolic stress, resulting from nutrient overload, leads to ER stress-mediated hepatocyte apoptosis[1, 8, 10, 11, 15-18]. Therefore, strategies to prevent ER stress-related hepatocyte death are highly desirable and would likely halt progression of NAFL to NASH.

Accumulating evidence suggests that C/EBP homologous protein (CHOP) is a major transcriptional regulator of ER stress-mediated apoptosis[19, 20]. Studies implicate CHOP in a wide-array of common diseases including neurodegenerative, cardiovascular, and metabolic disorders, including NAFLD[21-27]. Apart from modulating ER stress-mediated apoptosis, CHOP also plays a role in transcriptional regulation of cellular lipid metabolism[20, 28] suggesting that increased hepatic expression of CHOP in NAFLD patients may protect hepatocytes from FFA and cholesterol induced lipotoxicity. However, a mechanism whereby CHOP mediates protection against FFA-induced ER stress is not entirely clear.

We and others have demonstrated a beneficial role for glucagon-like peptide-1 (GLP-1) in *in vivo* and *in vitro* for NAFLD treatment[29-34]. GLP-1 is an incretin hormone secreted by the L-cells of the distal small intestine and proximal colon[35]. Prior data indicate that GLP-1 analogues can suppress FAA-induced steatosis in isolated hepatocytes, and in animal models of NASH fed a diet high in carbohydrate, saturated fat, and fructose. A recent small-scale double-blind placebo-controlled clinical trial in which the long-acting GLP-1 analogue, liraglutide was tested demonstrated liraglutide reduced metabolic dysfunction, increased hepatic insulin sensitivity, and reduced hepatic de novo lipogenesis (DNL) *in vivo*[36]. Studies in mice and cell culture models of steatosis demonstrate that GLP-1 agonists, liraglutide or exendin-4, protect steatotic hepatocytes from apoptosis by improved handling of FFA-induced ER stress[31, 34]. Here, by using global knock out mice for the critical ER stress protein, CHOP, we provide *in vivo* evidence that liraglutide mediates its protective effects through CHOP to ultimately prevent hepatocyte apoptosis and NAFLD progression. Our results demonstrate that in the absence of CHOP, liraglutide administration fails to

ameliorate steatohepatitis in mice fed a HFCD rendering hepatocytes far more susceptible to death.

MATERIALS AND METHODS

Mice

CHOP$^{-/-}$ mice on a C57BL/6 background were purchased from Jackson Laboratories (Bar Harbor, ME). Animals were housed in standard micro-isolator cages and maintained on a 12 h: 12 h light/dark cycle. All animals received humane care and all procedures were approved by the Institutional Animal Care and Use Committee of the Veterans' Administration Hospital in Decatur, GA.

Diet

Five week old age and weight matched adult male mice were fed a high fat, high cholesterol diet and high fructose diet (HFCD) containing 0.2% cholesterol, 20% protein, 43% CHO, 23% fat (6.6% trans-fat) and 2.31% fructose (TD.130885; Harlan Laboratories)[37, 38]; or the standard diet (ND) containing 16% protein, 61% carbohydrate and 7.2% fat. All cohorts were fed *ad libitum* for 16 weeks. After 12 weeks of feeding, mice received daily intraperitoneal injections of saline or liraglutide (200 μg/Kg body weight) for 4 weeks. Mice were weighed weekly and food intake per cage was also measured weekly. At the end of the 16 weeks, mice were fasted for 8 hours prior to euthanasia.

Histopathology and immunohistochemistry

Formalin-fixed liver tissues were paraffin-embedded, sectioned, and stained with H&E, Sirius Red, and Oil Red O as described previously[37]. Sirius Red stained areas were quantified by ImageJ software[39]. NASH scoring was performed by a liver pathologist using metrics for the NASH-CRN[40]. Apoptosis was detected using a terminal deoxynucleotidyl transferase dUTP nick end-labeling (TUNEL) assay as per the manufacturer's instructions (R&D Systems, Minneapolis, MN). For immunohistochemistry, paraffin-embedded liver tissue sections were probed with F4/80 antibody (eBiosciences, San Diego, Ca), followed by detection with HRP-conjugated secondary antibody and DAB substrate kit (Cell Signaling, Danvers, MA) following manufacturer's guidelines. Photomicrographs of histologic sections were obtained using a Zeiss Light Microscope (Zeiss, Jena, Germany).

Serological analysis

Blood obtained by cardiac puncture was collected for measurements of serum alanine aminotransferase (ALT), and aspartate aminotransferase (AST) concentrations using an AST and ALT Activity Assay Kit (Sigma-Aldrich, St. Louis, MO).

Quantitative real-time PCR

Isolation of total RNA from liver, cDNA synthesis and qRT-PCR were performed as previously described[41]. Expression data were normalized to 18S rRNA and data are presented as fold change in gene expression compared to WT- standard chow (ND) fed controls.

Glucose tolerance test (GTT) and insulin tolerance test (ITT)

GTTs and ITTs were performed at baseline, and after 16 weeks of HFCD feeding as described previously[30]. Blood glucose concentration was measured using a hand held glucometer (Freestyle Flash, Abbott Laboratories, Abbott Park, IL) as described elsewhere[30].

Immunoblotting

Liver tissues were homogenized and sonicated in RIPA lysis buffer (Sigma-Aldrich, St. Louis, MO) containing protease inhibitor cocktail and phosphostop (Roche Diagnostics, Indianapolis, IN), and total protein was extracted by centrifugation. A total of 30 μg protein was resolved on 4–12% precast SDS-PAGE gel (Invitrogen, Grand Island, NY) and transblotted onto a polyvinylidene fluoride membrane (Bio-Rad, Hercules, CA). Membranes were probed with antisera against p-JNK, JNK, p-PDK, PDK, p-AKT, AKT, p-PKCζ, PKCζ, p-PERK, PERK, p-elF2α, elF2α, p-IRE-1, IRE-1, GRP78, CHOP, caspase-3, cleaved caspase-3, ATF-6α, XBP-1, BCL-2, Bax, LC-3B and β-actin (Cell Signaling Technology, Danvers, MA). Isotype-matched horseradish peroxidase conjugated secondary antibodies, enhanced chemiluminescence substrate (Pierce, Rockford, IL) and a FluorChem 8900 digital imaging system (AlphaInnotech, San Leandro, CA) were used to visualize protein bands. Densitometric analyses was performed with VisionWorks® Software, version 6.8 (UVP, Upland, CA).

Hepatic hydroxyproline quantification:

Hepatic 4-hydroxyproline concentration was quantified using the Hydroxyproline Assay kit (Sigma-Aldrich, St. Louis, MO) following manufacturer's guidelines.

Primary mouse hepatocyte isolation and *in vivo* fatty acid and exendin-4 treatment

Primary mouse hepatocytes from 8 weeks old WT and *CHOP*$^{-/-}$ mice were isolated as previously described[42]. Isolated hepatocytes were cultured in William's medium E Formulation (Sigma-Aldrich, St. Louis, MO) supplemented with 10% fetal bovine serum (FBS; Atlanta Biologicals, Flowery Branch, GA) and 5% Penicillin-Streptomycin (Sigma-Aldrich, St. Louis, MO). The *in vitro* fatty acid and exendin-4 treatments were performed as described previously[31]. Hepatocytes were pretreated with 400 μM palmitic acid (PA) in ethanol (EtOH) for 24 h, after which hepatocytes were treated with 10 nM exendin-4 and PA for an additional 24 hr. Hepatocytes treated with EtOH (Control), or EtOH plus exendin-4 (Control + Ex4), or PA alone were used as controls. At the end of the experiment, cells were subjected to RNA isolation or Oil Red O staining as described above. Gene expression data were normalized to GAPDH and data are presented as fold change in gene expression compared to WT + EtOH controls.

Statistical analysis

Values were reported as means ± SEM and each treatment group included 5-7 mice. All experiments were repeated at least two times on two separate occasions. Data were analyzed by analysis of variance (ANOVA) with Bonferroni's post hoc test for determination of statistical significance ($p < 0.05$).

RESULTS

Liraglutide treatment attenuates steatohepatitis in HFCD-fed WT mice

We have previously demonstrated that liraglutide treatment significantly reduced steatosis in WT mice fed a high fat and high sugar diet (HFD)[30-34]. We recently reported that mice fed 0.2% cholesterol in addition to HFD (HFCD) for 16 weeks resulted in mild steatohepatitis characterized by steatosis, inflammation, and mild fibrosis[37]. Here, we first determined whether liraglutide treatment would also be effective in suppressing steatohepatitis in HFCD-fed mice. As shown in Fig. 1A-M, WT mice fed the HFCD for 16 weeks developed histological features of steatohepatitis indicated by ballooning degeneration of hepatocytes, inflammatory cell infiltration, and sinusoidal fibrosis. In agreement with previous reports[30-34], four weeks of liraglutide treatment significantly reduced hepatic steatosis, body weight, and both liver and visceral fat weight expressed as percent of body weight (Fig. 1A-F). Liraglutide treatment also significantly reduced the NASH-CRN histology score[43], hepatic hydroxyproline levels and serum AST and ALT levels (Fig 1G-J).

CHOP modulates liraglutide-mediated suppression of steatohepatitis

As anticipated, CHOP expression was markedly increased in HFCD-fed WT mice, and the daily administration of liraglutide suppressed CHOP expression (Fig. 6A,H). Therefore, we investigated whether CHOP was pivotal in liraglutide-mediated suppression of steatohepatitis. Consistent with previous observations[44], HFCD-fed *CHOP*$^{-/-}$ mice developed more severe histological features of NASH compared with HFCD-fed WT mice (Fig. 1A-C, G & 2A-C, G). HFCD-fed *CHOP*$^{-/-}$ mice gained greater body weight, and had greater liver weight and visceral fat weight compared with HFCD-fed WT mice (Fig. 1D-F & 2D-F). HFCD-fed *CHOP*$^{-/-}$ mice had higher hepatic fibrosis compared with HFCD-fed WT mice (Fig. 1K-M & 2K-M). In addition, hepatic inflammation in HFCD-fed *CHOP*$^{-/-}$ mice was higher than HFCD-fed WT mice as evidenced by increased infiltration of macrophages, increase in tumor necrosis factor (TNF)-α and monocyte chemoattractant protein (MCP)-1 transcript levels, and higher serum AST and ATL levels (Fig. 3A-C & 2A, G, M). Liraglutide treatment attenuated steatosis, and hepatic inflammation in the HFCD-fed *CHOP*$^{-/-}$ mice, but this effect was far less robust compared to the liraglutide treated HFCD-fed WT mouse cohort (Fig. 1A-M; 2A-M & 3A-C). Taken together, these data suggest that CHOP serves to protect mouse liver from HFCD-mediated hepatic inflammation. Also, that CHOP plays an essential role in liraglutide-mediated protection from NASH-associated liver injury.

HFCD-fed CHOP$^{-/-}$ mice are resistant to liraglutide-mediated improvement in insulin sensitivity and glucose homeostasis

We and others have previously demonstrated that liraglutide treatment attenuates steatosis by improving hepatic insulin sensitivity in both *in vitro* and *in vivo* models of hepatic steatosis[30-34]. Since CHOP plays a role in suppressing metabolic genes during ER stress[20, 28], we tested whether liraglutide improves insulin sensitivity in the absence of CHOP. As seen in Fig 4A-D, liraglutide treatment significantly improved hyperglycemia and insulin sensitivity in HFCD-fed WT mice. However, HFCD-fed *CHOP*$^{-/-}$ mice remained insulin resistant and hyperglycemic despite 4 weeks of liraglutide treatment (Fig. 4A-D). To

determine the molecular mechanisms that could account for persistent insulin resistance in the *CHOP*$^{-/-}$ mice, we performed a detailed analysis of the downstream mediators of the insulin-signaling pathway. As shown in Fig. 4E-J, we demonstrated that activation of PDK, AKT and PKCζ were significantly attenuated in both WT and *CHOP*$^{-/-}$ mice fed HFCD. Although we did not observe any significant differences in JNK activation between ND and HFCD fed WT mice, HFCD significantly increased JNK activation in *CHOP*$^{-/-}$ mice, which also correlated with impaired insulin sensitivity in these mice (Fig. 4E,G). In agreement with our previous *in vitro* results[34], liraglutide treatment significantly activated PDK, AKT, and PKCζ and reduced JNK activation in HFCD-fed WT mice (Fig. 4E-J). Interestingly, liraglutide treatment also induced activation of PDK, AKT and PKCζ in HFCD-fed *CHOP*$^{-/-}$ mice. However liraglutide administration in *CHOP*$^{-/-}$ mice failed to suppress JNK activation; and, while insulin signaling elements were activated, glucose handling in the *CHOP*$^{-/-}$ mice fed the HFCD was not improved.

Liraglutide treatment fails to improve lipid, cholesterol and glucose metabolism in the absence of CHOP

Next, to understand the discrepancy between insulin signaling pathway activation and failure to improve glucose handling following liraglutide administration in *CHOP*$^{-/-}$ mice, we investigated the effect of liraglutide on key mediators of lipid, cholesterol and glucose metabolism. As seen in Fig. 5A-D, HFCD significantly increased peroxisomal β-oxidation and uptake of long chain fatty acids as indicated by increased expression of Carnitine palmitoyltransferase (CPT)-1α, Acyl-CoA oxidase (ACOX)-1 and ACOX-2, key mediators of peroxisomal β-oxidation, in WT HFCD-fed mice. HFCD also increased CPT-1α and ACOX-2 expression in *CHOP*$^{-/-}$ mice, however the expression level was significantly lower than the WT mice (Fig. 5A-D). Liraglutide treatment suppressed β-oxidation in HFCD-fed WT mice as indicated by increased peroxisome proliferator-activated receptor (PPAR)-α expression and decrease in CPT-1α, ACOX-1 and ACOX-2 expression. None of these key transcription factors and enzymes associated with β-oxidation were suppressed in the liraglutide administered HFCD-fed *CHOP*$^{-/-}$ mice, nor was PPARα increased, suggesting that CHOP is required for liraglutide-mediated suppression of β-oxidation (Fig. 5A-D).

In contrast to β-oxidation, expression levels of sterol regulatory element-binding protein (SREBP)-1c, PPAR-γ, fatty acid synthase (FAS) and carbohydrate-responsive element-binding protein (ChREBP), key mediators of *de novo* lipogenesis and carbohydrate metabolism, were significantly higher in HFCD-fed *CHOP*$^{-/-}$ mice suggesting a role of CHOP in regulating carbohydrate and fat metabolism (Fig. 5E-H). Liraglutide treatment suppressed *de novo* lipogenesis in both WT and *CHOP*$^{-/-}$ mice fed HFCD as indicated by reduced expression of PPAR-γ and FASN (Fig. 5E-H). Interestingly, liraglutide failed to suppress SREBP1c and ChREBP in HFCD-fed *CHOP*$^{-/-}$ mice suggesting that CHOP may play a role in Liraglutide-mediated suppression of glucose metabolism. Taken together, these data suggest that CHOP is required for liraglutide-mediated improvement in lipid, cholesterol, and glucose metabolism even though key players of the hepatocyte insulin signaling pathway were activated in both WT and the *CHOP*$^{-/-}$ mice fed the HFCD.

Liraglutide treatment attenuates ER stress in HFCD-fed WT mice but not in CHOP$^{-/-}$ mice

Since hepatic ER stress contributes to the development of steatosis[10, 11, 15, 17, 45], we investigated whether liraglutide treatment attenuates steatohepatitis by suppressing ER stress in the absence of CHOP. As shown in Fig 6A-H, HFCD significantly activated PKR like ER kinase (PERK) and inositol requiring 1 (IRE-1) pathways, as indicated by increased phosphorylation of PERK and its downstream effector E74-like factor 2a (elF2a), and IRE-1 and its downstream effector X-box binding protein (XBP)-1, respectively, in WT mice. HFCD also increased activation of activating transcription factor (ATF)-6α in WT mice. Similarly all three key UPR pathways were also significantly activated in the HFCD-fed *CHOP*$^{-/-}$ mice (Fig. 6A-H). However, in the absence of CHOP, HFCD induced significantly higher activation of PERK, IRE-1 and ATF-6α pathways compared to WT control (Fig. 6A-H). Liraglutide treatment attenuated HFCD-induced activation of PERK and IRE-1 pathways in WT mice suggesting that liraglutide treatment improved ER homeostasis. However, in the HFCD-fed *CHOP*$^{-/-}$ mice, liraglutide treatment was ineffective in suppressing elF2 and IRE-1 activation, which could account for why liraglutide failed to suppress ER stress in the absence of CHOP. It should be noted that increased activation of IRE-1 in HFCD-fed *CHOP*$^{-/-}$ mice did not increase XBP-1 activation in these mice. Furthermore, liraglutide treatment significantly increased XBP-1 activation in both WT and *CHOP*$^{-/-}$ mice fed HFCD; however, this increase did not correlate with liraglutide-mediated decrease in IRE-1 activation in these mice. We also did not observe any significant differences in GRP78 expression between WT and *CHOP*$^{-/-}$ mice fed HFCD; nor did liraglutide treatment affect GRP78 expression in WT mice fed HFCD (Fig. 6A,E). However, liraglutide treatment significantly increased GRP78 expression in the HFCD-fed *CHOP*$^{-/-}$ mice. HFCD-induced ER stress in WT mice correlated with increased expression of CHOP, and liraglutide treatment significantly reduced CHOP expression (Fig. 6A,H). Taken together, these data suggest that liraglutide treatment attenuated HFCD-induced hepatic injury by suppressing ER stress, and implicate a central role for CHOP in protecting hepatocytes from HFCD-induced ER stress.

Liraglutide treatment suppresses hepatic apoptosis in HFCD-fed WT mice but not in CHOP$^{-/-}$ mice

Since CHOP plays a role in ER stress-induced apoptosis, and liraglutide treatment has been shown to suppress lipotoxicity-induced hepatocyte apoptosis[15, 17], we next investigated whether liraglutide treatment was equally effective in suppressing apoptosis in the absence of CHOP. As seen in Fig 7A-F, the HFCD increased hepatocyte apoptosis in both WT and *CHOP*$^{-/-}$ mice indicated by increased number of TUNEL positive cells and caspase-3 activation in the liver. However, the absence of CHOP resulted in significantly higher apoptosis in HFCD-fed *CHOP*$^{-/-}$ mice compared with WT controls (Fig. 7A). Higher apoptosis in HFCD-fed CHOP$^{-/-}$ mice correlated with increased Bax and LC-3B expression, and decreased BCL-2 expression (Fig. 7B-F). Liraglutide treatment reduced apoptosis in both WT and *CHOP*$^{-/-}$ mice fed HFCD, however apoptosis remained significantly higher in liraglutide treated HFCD-fed *CHOP*$^{-/-}$ mice compared with WT mice fed HFCD (Fig. 7A). While liraglutide treatment significantly lowered caspase-3 activation in *CHOP*$^{-/-}$ mice, it did not reduce Bax and LC-3B expression in this cohort (Fig. 7B-F).

Taken together, these data suggest that CHOP is critical for liraglutide-mediated suppression of diet-induced hepatocyte death.

GLP-1 analog exendin-4 attenuates fatty acid deposition in primary hepatocytes from WT mice but not in primary hepatocytes from CHOP$^{-/-}$ mice.

To investigate whether the role of CHOP in modulating liraglutide-mediated protection from NASH *in vivo* is hepatocyte specific, primary liver hepatocytes isolated from WT and *CHOP*$^{-/-}$ mice were cultured in 400 μM PA palmitic acid (PA) and treated with 10 nM exendin-4. As seen in Fig. 8A, PA treatment significantly increased fat deposition in both WT and *CHOP*$^{-/-}$ hepatocytes indicated by increased Oil Red O stained fat droplets in the hepatocytes. It should be noted that fat deposition in the *CHOP*$^{-/-}$ hepatocytes treated with ethanol alone was higher compared with WT hepatocytes treated with ethanol (Fig. 8A). Exendin-4 reduced fat deposition in the PA treated WT hepatocytes, but failed to reduce fat deposition in PA treated *CHOP*$^{-/-}$ hepatocytes (Fig. 8A). Further analysis revealed that PA treatment significantly increased peroxisomal β-oxidation and uptake of long chain fatty acids as indicated by increased expression of CPT-1α, and ACOX-1 transcripts in both WT and *CHOP*$^{-/-}$ hepatocytes (Fig. 8B-C). Exendin-4 treatment suppressed β-oxidation in PA treated WT hepatocytes, however did not suppress β-oxidation and fatty acid uptake in the PA treated *CHOP*$^{-/-}$ hepatocytes (Fig. 8B-C). Additionally, exendin-4 also failed to suppress *de novo* lipogenesis and glucose metabolism in the absence of CHOP as indicated by significantly higher expression of FAS and SREBP1c transcripts in PA + Ex4 treated *CHOP*$^{-/-}$ hepatocytes (Fig. 8D-E). Together these data support our *in vivo* observations and demonstrate that CHOP plays a role in modulating GLP-1 mediated protection from fat deposition in hepatocytes.

Discussion

In the present study, we demonstrate a critical role for CHOP in regulating diet-induced ER stress in the setting of administration of the long-acting GLP-1 analogue liraglutide *in vivo*, along with confirmatory *in vitro* studies in primary hepatocytes derived from *CHOP*$^{-/-}$ mice. Here, we show that CHOP plays a protective role in reducing ER stress-induced hepatocyte apoptosis, and is essential for the action of liraglutide in mediating these events during nutrient excess. Furthermore, our results demonstrate the contribution of liraglutide mediation of cell carbohydrate and lipid metabolism in preventing disease progression.

CHOP is a bZIP-containing transcription factor, and is a common point of molecular convergence for all three canonical ER stress transducers, IRE1, PERK, and ATF6[46, 47]. CHOP is among the highly inducible genes during ER stress and its expression is primarily regulated at the transcriptional level by various components of the UPR pathway[20, 48]. CHOP is primarily considered a pro-apoptotic transcription factor that mediates ER stress-induced cell death through the regulation of the Bcl-2 family of proteins[46]. Consequently, CHOP deficiency provides partial resistance to ER stress-mediated apoptosis in *in vivo* models of chemically induced ER stress[46, 47]. However, paradoxically, in our model of nutrient excess, the results indicate that CHOP plays a protective role, and not a deleterious one, in restoring ER homeostasis.

Despite the ongoing controversy surrounding the expression of GLP-1 receptor in the liver, studies conducted in our laboratory, and others, substantiate a direct role for GLP-1 receptor agonists in suppressing hepatic steatosis in both cell culture and animal models[29-31, 34]. It is now well-established that GLP-1 receptor agonists suppress hepatic accumulation of triglycerides not only by promoting insulin sensitivity in fat-loaded hepatocytes, but also by restoring ER homeostasis and reducing subsequent lipotoxicity-mediated hepatocyte death[29-31, 34]. In agreement with these previous reports, liraglutide administration protected WT mice from HFCD-induced steatohepatitis. However, liraglutide treatment did not have a significant effect on HFCD-induced steatohepatitis in *CHOP*$^{-/-}$ mice. Liraglutide treatment, in the absence of CHOP failed to protect the deleterious effects of HFCD-induced liver injury and cell death, strongly suggesting that CHOP plays a direct role in liraglutide-mediated protection from HFCD-induced steatohepatitis. Our results are substantiated by *in vitro* findings of primary hepatocytes derived from *CHOP*$^{-/-}$ mice, which demonstrate that GLP-1 analogues must play a role in modulating carbohydrate and lipid metabolism in the hepatocyte.

Apart from modulating ER stress associated apoptosis, CHOP also regulates carbohydrate and lipid metabolism by modulating transcriptional control of master regulators of glucose metabolism, fatty acid synthesis, and cholesterol metabolism[20, 28]. Our data demonstrate a relationship between liraglutide administration and CHOP mediated regulation of key genes associated with hepatocyte metabolism in the setting of a Western diet (HFCD). In the HFCD-fed *CHOP*$^{-/-}$ cohort, liraglutide administration failed to repress β-oxidation, and transcriptional regulators of *de novo* lipogenesis and cholesterol metabolism suggesting CHOP functions as a transcriptional repressor of metabolic genes during HFCD-induced ER stress. Taken together, these data suggest that CHOP plays a major role in the liraglutide-mediated transcriptional regulation of hepatic metabolism during nutrient excess. Our findings provide a molecular framework in support of the recently reported small-scale clinical trial, which demonstrated liraglutide reduced hepatic insulin resistance and *de novo* lipogenesis[16].

Apart from its insulinotropic effect, GLP-1 analogs also increase insulin sensitivity and glucose uptake by skeletal muscle, hepatocytes, and adipose tissue[30, 34, 49]. Our results confirm liraglutide- mediated improvement in insulin sensitivity in HFCD-fed WT mice, but this was not true in the *CHOP*$^{-/-}$ mice fed the HFCD. These data provide additional evidence for a role of CHOP in regulating glucose and more importantly fatty acid metabolism. While the insulin signaling pathway was activated in mice given liraglutide in the setting of the Western diet, only WT mice had restored glucose tolerance, not the *CHOP*$^{-/-}$ mice. As anticipated the WT mice fed the Western diet had a reduction in JNK. That alone could explain why there is less caspase-3 activation and reduced TUNEL staining. This was not the case for the *CHOP*$^{-/-}$ mice. In both HFCD-fed *CHOP*$^{-/-}$ cohorts, JNK activity was unchanged, yet caspase-3 activity and TUNEL staining were suppressed in the *CHOP*$^{-/-}$ mice fed the HFCD upon liraglutide administration. This would imply that either CHOP regulates the insulin pathway downstream of PDK-1, AKT and PKC-ζ, or that CHOP functions to suppress *de novo* lipogenesis. A reduction in *de novo* lipogenesis would explain reduced lipotoxicity, reduced hepatic inflammation, and ultimately reduced hepatocyte apoptosis.

The implication that CHOP is involved in ER stress-induced lipotoxicity stems from strong correlational data in NAFLD[50]. However, rather than attenuating disease progression, genetic ablation of CHOP accelerates NAFLD progression in both HFD and methionine and choline deficient models of NASH[44, 51]. The ability of CHOP to transcriptionally modulate fatty acid metabolism may explain its apparent paradoxical protective role during chronic nutrient excess conditions[20, 28]. This conclusion is consistent with our data showing that liraglutide fails to promote insulin sensitivity, reduce steatosis, restore ER homeostasis and reduce subsequent lipotoxicity-mediated hepatocyte death in the absence of CHOP. Increased hepatocyte death in HFCD-fed *CHOP*$^{-/-}$ mice can be attributed to lower expression of anti-apoptotic protein BCL-2 and higher expression of Bax and LC-3B in these mice. In the *CHOP*$^{-/-}$ mice, liraglutide administration reduced ER stress-related proteins, but not to the level of the WT mice fed the HFCD. Liraglutide treatment also reduced caspase-3 activation in HFCD-fed CHOP$^{-/-}$ mice but this did not correlate with a decrease in TUNEL positive cells suggesting that another pathway *in vivo* must account for higher hepatocyte apoptosis following liraglutide administration. The increased expression of Bax and LC-3B in HFCD-fed *CHOP*$^{-/-}$ mice and inability of liraglutide to attenuate apoptosis by reducing Bax and LC-3B levels in the absence of caspase-3 activation implies that both caspase dependent and independent cell death pathways are at play in the HFCD-fed *CHOP*$^{-/-}$ mice. Future studies will be required to clarify the mechanisms of caspase independent cell death pathways.

In summary, our data indicate that *in vivo* the administration of liraglutide may be protective against NAFLD disease progression by initially reducing *de novo* lipogenesis and thus reducing lipotoxicity. As clinical trials continue, further clarification for the molecular mechanisms accounting for the pleotropic role of long-acting GLP-1 analogues in the liver is warranted.

Acknowledgments

Funding: This work was supported by NIH grant DK062092, VA grant I01BX001746, and funds from Emory University School of Medicine, to FAA.

Abbreviations

NAFLD	non-alcoholic fatty liver disease
NASH	non-alcoholic steatohepatitis
CHOP	CCAAT/enhancer-binding protein homologous protein

References

1. Wree A, Broderick L, Canbay A, et al. From NAFLD to NASH to cirrhosis-new insights into disease mechanisms. Nature reviews Gastroenterology & hepatology. 2013; 10(11):627–636. [PubMed: 23958599]
2. Mahady SE, George J. Management of nonalcoholic steatohepatitis: an evidence-based approach. Clinics in liver disease. 2012; 16(3):631–645. [PubMed: 22824485]
3. Adams LA, Lymp JF, St Sauver J, et al. The natural history of nonalcoholic fatty liver disease: a population-based cohort study. Gastroenterology. 2005; 129(1):113–121. [PubMed: 16012941]

4. O'Grady MJaC, JC. Assessing the Economics of Obesity and Obesity Interventions. print copy in press 2012. Available from: http://obesitycampaign.org/documents/StudyAssessingtheEconomicsofObesityandObesityIntervention.pdf
5. Williams CD, Stengel J, Asike MI, et al. Prevalence of nonalcoholic fatty liver disease and nonalcoholic steatohepatitis among a largely middle-aged population utilizing ultrasound and liver biopsy: a prospective study. Gastroenterology. 2011; 140(1):124–131. [PubMed: 20858492]
6. Tetri LH, Basaranoglu M, Brunt EM, et al. Severe NAFLD with hepatic necroinflammatory changes in mice fed trans fats and a high-fructose corn syrup equivalent. American journal of physiology Gastrointestinal and liver physiology. 2008; 295(5):G987–995. [PubMed: 18772365]
7. Neuschwander-Tetri BA. Hepatic lipotoxicity and the pathogenesis of nonalcoholic steatohepatitis: the central role of nontriglyceride fatty acid metabolites. Hepatology. 2010; 52(2):774–788. [PubMed: 20683968]
8. Malhi H, Gores GJ. Molecular mechanisms of lipotoxicity in nonalcoholic fatty liver disease. Seminars in liver disease. 2008; 28(4):360–369. [PubMed: 18956292]
9. Li J, Huang J, Li JS, et al. Accumulation of endoplasmic reticulum stress and lipogenesis in the liver through generational effects of high fat diets. J Hepatol. 2012; 56(4):900–907. [PubMed: 22173165]
10. Zhou H, Liu R. ER stress and hepatic lipid metabolism. Front Genet. 2014; 5:112. [PubMed: 24847353]
11. Malhi H, Kaufman RJ. Endoplasmic reticulum stress in liver disease. J Hepatol. 2011; 54(4):795–809. [PubMed: 21145844]
12. Xu C, Bailly-Maitre B, Reed JC. Endoplasmic reticulum stress: cell life and death decisions. J Clin Invest. 2005; 115(10):2656–2664. [PubMed: 16200199]
13. Walter P, Ron D. The unfolded protein response: from stress pathway to homeostatic regulation. Science. 2011; 334(6059):1081–1086. [PubMed: 22116877]
14. Li Y, Ge M, Ciani L, et al. Enrichment of endoplasmic reticulum with cholesterol inhibits sarcoplasmic-endoplasmic reticulum calcium ATPase-2b activity in parallel with increased order of membrane lipids: implications for depletion of endoplasmic reticulum calcium stores and apoptosis in cholesterol-loaded macrophages. The Journal of biological chemistry. 2004; 279(35): 37030–37039. [PubMed: 15215242]
15. Oyadomari S, Harding HP, Zhang Y, et al. Dephosphorylation of translation initiation factor 2alpha enhances glucose tolerance and attenuates hepatosteatosis in mice. Cell Metab. 2008; 7(6):520–532. [PubMed: 18522833]
16. Ozcan U, Cao Q, Yilmaz E, et al. Endoplasmic reticulum stress links obesity, insulin action, and type 2 diabetes. Science. 2004; 306(5695):457–461. [PubMed: 15486293]
17. Wang D, Wei Y, Pagliassotti MJ. Saturated fatty acids promote endoplasmic reticulum stress and liver injury in rats with hepatic steatosis. Endocrinology. 2006; 147(2):943–951. [PubMed: 16269465]
18. Cnop M, Foufelle F, Velloso LA. Endoplasmic reticulum stress, obesity and diabetes. Trends Mol Med. 2012; 18(1):59–68. [PubMed: 21889406]
19. Szegezdi E, Logue SE, Gorman AM, et al. Mediators of endoplasmic reticulum stress-induced apoptosis. EMBO Rep. 2006; 7(9):880–885. [PubMed: 16953201]
20. Chikka MR, McCabe DD, Tyra HM, et al. C/EBP homologous protein (CHOP) contributes to suppression of metabolic genes during endoplasmic reticulum stress in the liver. The Journal of biological chemistry. 2013; 288(6):4405–4415. [PubMed: 23281479]
21. Oyadomari S, Koizumi A, Takeda K, et al. Targeted disruption of the Chop gene delays endoplasmic reticulum stress-mediated diabetes. J Clin Invest. 2002; 109(4):525–532. [PubMed: 11854325]
22. Song B, Scheuner D, Ron D, et al. Chop deletion reduces oxidative stress, improves beta cell function, and promotes cell survival in multiple mouse models of diabetes. J Clin Invest. 2008; 118(10):3378–3389. [PubMed: 18776938]
23. Ji C, Mehrian-Shai R, Chan C, et al. Role of CHOP in hepatic apoptosis in the murine model of intragastric ethanol feeding. Alcohol Clin Exp Res. 2005; 29(8):1496–1503. [PubMed: 16131858]

24. Silva RM, Ries V, Oo TF, et al. CHOP/GADD153 is a mediator of apoptotic death in substantia nigra dopamine neurons in an in vivo neurotoxin model of parkinsonism. J Neurochem. 2005; 95(4):974–986. [PubMed: 16135078]
25. Namba T, Tanaka K, Ito Y, et al. Positive role of CCAAT/enhancer-binding protein homologous protein, a transcription factor involved in the endoplasmic reticulum stress response in the development of colitis. Am J Pathol. 2009; 174(5):1786–1798. [PubMed: 19359519]
26. Thorp E, Li G, Seimon TA, et al. Reduced apoptosis and plaque necrosis in advanced atherosclerotic lesions of Apoe−/− and Ldlr−/− mice lacking CHOP. Cell Metab. 2009; 9(5):474–481. [PubMed: 19416717]
27. Tsukano H, Gotoh T, Endo M, et al. The endoplasmic reticulum stress-C/EBP homologous protein pathway-mediated apoptosis in macrophages contributes to the instability of atherosclerotic plaques. Arterioscler Thromb Vasc Biol. 2010; 30(10):1925–1932. [PubMed: 20651282]
28. Rutkowski DT, Wu J, Back SH, et al. UPR pathways combine to prevent hepatic steatosis caused by ER stress-mediated suppression of transcriptional master regulators. Dev Cell. 2008; 15(6): 829–840. [PubMed: 19081072]
29. Yang J, Ao N, Du J, et al. Protective effect of liraglutide against ER stress in the liver of high-fat diet-induced insulin-resistant rats. Endocrine. 2015; 49(1):106–118. [PubMed: 25471281]
30. Mells JE, Fu PP, Sharma S, et al. Glp-1 analog, liraglutide, ameliorates hepatic steatosis and cardiac hypertrophy in C57BL/6J mice fed a Western diet. American journal of physiology Gastrointestinal and liver physiology. 2012; 302(2):G225–235. [PubMed: 22038829]
31. Sharma S, Mells JE, Fu PP, et al. PloS one. 2011; 6(9):e25269. [PubMed: 21957486]
32. Liu Y, Wei R, Hong TP. Potential roles of glucagon-like peptide-1-based therapies in treating non-alcoholic fatty liver disease. World J Gastroenterol. 2014; 20(27):9090–9097. [PubMed: 25083081]
33. Ao N, Yang J, Wang X, et al. Glucagon-like peptide-1 preserves non-alcoholic fatty liver disease through inhibition of the endoplasmic reticulum stress-associated pathway. Hepatol Res. 2015
34. Gupta NA, Mells J, Dunham RM, et al. Glucagon-like peptide-1 receptor is present on human hepatocytes and has a direct role in decreasing hepatic steatosis in vitro by modulating elements of the insulin signaling pathway. Hepatology. 2010; 51(5):1584–1592. [PubMed: 20225248]
35. Drucker DJ. Minireview: the glucagon-like peptides. Endocrinology. 2001; 142(2):521–527. [PubMed: 11159819]
36. Armstrong MJ, Hull D, Guo K, et al. Glucagon-like peptide 1 decreases lipotoxicity in non-alcoholic steatohepatitis. J Hepatol. 2016; 64(2):399–408. [PubMed: 26394161]
37. Mells JE, Fu PP, Kumar P, et al. Saturated fat and cholesterol are critical to inducing murine metabolic syndrome with robust nonalcoholic steatohepatitis. The Journal of nutritional biochemistry. 2014
38. Charlton M, Krishnan A, Viker K, et al. Fast food diet mouse: novel small animal model of NASH with ballooning, progressive fibrosis, and high physiological fidelity to the human condition. American journal of physiology Gastrointestinal and liver physiology. 2011; 301(5):G825–834. [PubMed: 21836057]
39. Schneider CA, Rasband WS, Eliceiri KW. NIH Image to ImageJ: 25 years of image analysis. Nat Methods. 2012; 9(7):671–675. [PubMed: 22930834]
40. Kleiner DE, Brunt EM, Van Natta M, et al. Design and validation of a histological scoring system for nonalcoholic fatty liver disease. Hepatology. 2005; 41(6):1313–1321. [PubMed: 15915461]
41. Kumar P, Smith T, Rahman K, et al. Adiponectin agonist ADP355 attenuates CCl4-induced liver fibrosis in mice. PloS one. 2014; 9(10):e110405. [PubMed: 25310107]
42. Severgnini M, Sherman J, Sehgal A, et al. A rapid two-step method for isolation of functional primary mouse hepatocytes: cell characterization and asialoglycoprotein receptor based assay development. Cytotechnology. 2012; 64(2):187–195. [PubMed: 22105762]
43. Brunt EM, Kleiner DE, Wilson LA, et al. Nonalcoholic fatty liver disease (NAFLD) activity score and the histopathologic diagnosis in NAFLD: distinct clinicopathologic meanings. Hepatology. 2011; 53(3):810–820. [PubMed: 21319198]

44. Malhi H, Kropp EM, Clavo VF, et al. C/EBP homologous protein-induced macrophage apoptosis protects mice from steatohepatitis. The Journal of biological chemistry. 2013; 288(26):18624–18642. [PubMed: 23720735]

45. Jo H, Choe SS, Shin KC, et al. Endoplasmic reticulum stress induces hepatic steatosis via increased expression of the hepatic very low-density lipoprotein receptor. Hepatology. 2013; 57(4): 1366–1377. [PubMed: 23152128]

46. Li Y, Guo Y, Tang J, et al. New insights into the roles of CHOP-induced apoptosis in ER stress. Acta Biochim Biophys Sin (Shanghai). 2014; 46(8):629–640. [PubMed: 25016584]

47. Oyadomari S, Mori M. Roles of CHOP/GADD153 in endoplasmic reticulum stress. Cell Death Differ. 2004; 11(4):381–389. [PubMed: 14685163]

48. Okada T, Yoshida H, Akazawa R, et al. Distinct roles of activating transcription factor 6 (ATF6) and double-stranded RNA-activated protein kinase-like endoplasmic reticulum kinase (PERK) in transcription during the mammalian unfolded protein response. The Biochemical journal. 2002; 366:585–594. Pt 2. [PubMed: 12014989]

49. Ayala JE, Bracy DP, James FD, et al. The glucagon-like peptide-1 receptor regulates endogenous glucose production and muscle glucose uptake independent of its incretin action. Endocrinology. 2009; 150(3):1155–1164. [PubMed: 19008308]

50. Ibrahim SH, Kohli R, Gores GJ. Mechanisms of lipotoxicity in NAFLD and clinical implications. J Pediatr Gastroenterol Nutr. 2011; 53(2):131–140. [PubMed: 21629127]

51. Soon RK Jr. Yan JS, Grenert JP, et al. Stress signaling in the methionine-choline-deficient model of murine fatty liver disease. Gastroenterology. 2010; 139(5):1730–1739. 1739 e1731. [PubMed: 20682321]

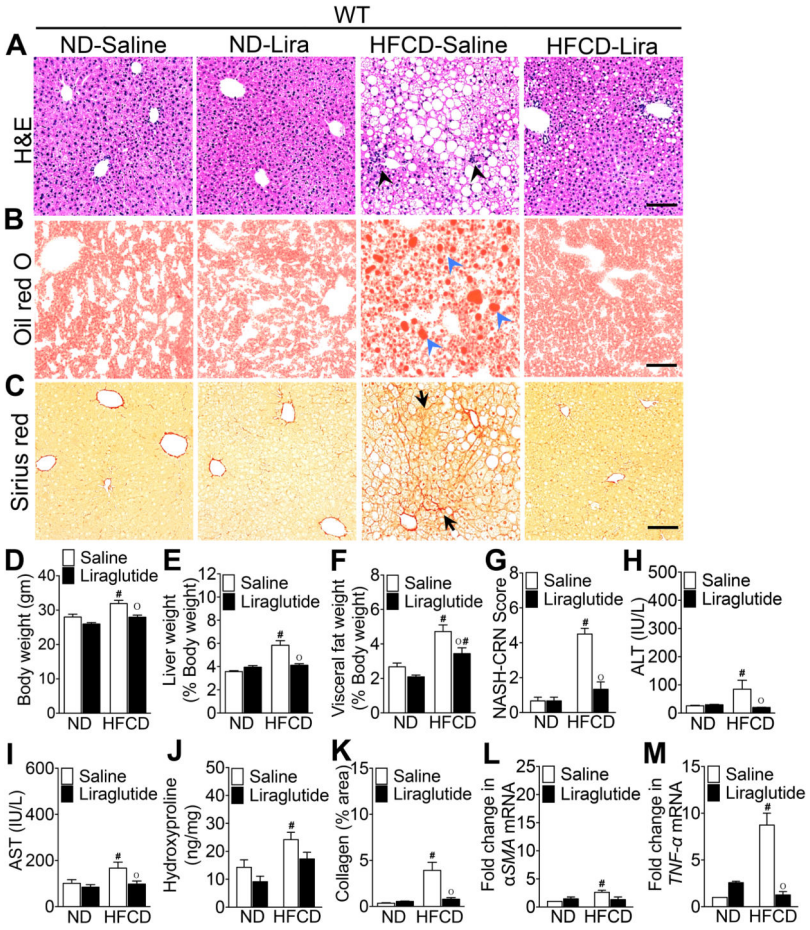

Figure 1. Liraglutide treatment attenuates steatohepatitis in HFCD-fed WT mice

Photomicrographs of (A) Hematoxylin and Eosin, (B) Oil Red O, and (C) Sirius Red stained liver sections of WT mice fed a ND or HFCD for 16 weeks. After 12 weeks of feeding, mice received daily injections of saline or liraglutide (Lira) for 4 weeks. Black arrowheads, inflammatory immune cells; blue arrowheads, fat droplets; black arrows, collagen deposition. (D) Body, (E) liver, and (F) visceral fat weight as well as (G) NASH-CRN score, serum (H) ALT and (I) AST levels, and (J) hepatic hydroxyproline levels measured at the end of the 16 week experiments. Changes in liver and visceral fat weights are reported as percentages of body weight. (K) Quantitative analysis of Sirius Red stained liver tissue sections. Quantitative RT-PCR analysis of hepatic (L) αSMA and (M) TNF-α transcript levels measured at the end of the 16 week experiments. Data are presented as mean ± SEM; n = 5-7 mice per group. Hashtags indicate significant differences ($p < 0.05$) between ND- or HFCD-fed WT mice. “o” indicates significant differences ($p < 0.05$) between saline or liraglutide-treated WT mice. Scale 20 μm.

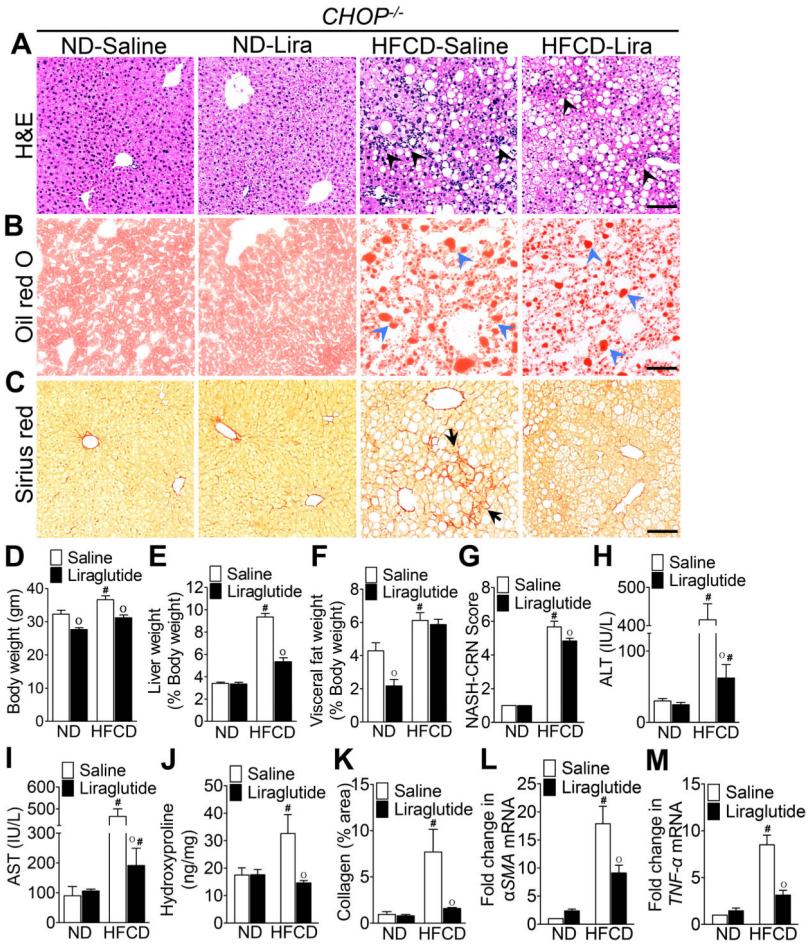

Figure 2. CHOP modulates liraglutide-mediated suppression of steatohepatitis

Photomicrogaphs of (A) Hematoxylin and Eosin, (B) Oil Red O, and (C) Sirius Red stained liver tissue sections of *CHOP*$^{-/-}$ mice fed a ND or HFCD for 16 weeks. After 12 weeks of feeding, mice received daily injections of saline or liraglutide (Lira) for 4 weeks. Black arrowheads, inflammatory immune cells; blue arrowheads, fat droplets; black arrows, collagen deposition. (D) Body, (E) liver, and (F) visceral fat weight as well as (G) NASH-CRN score, serum (H) ALT and (I) AST levels, and (J) hepatic hydroxyproline levels measured at the end of the 16 week experiments. Changes in liver and visceral fat weights are reported as percentages of body weight. (K) Quantitative analysis of Sirius Red stained liver tissue sections. Quantitative RT-PCR analysis of hepatic (L) αSMA and (M) TNF-α transcript levels measured at the end of the 16 week experiments. Data are presented as mean ± SEM; n = 5-7 mice per group. Hashtags indicate significant differences ($p < 0.05$) between ND- or HFCD-fed WT mice. “o” indicates significant differences ($p < 0.05$) between saline or liraglutide-treated WT mice. Scale 20 μm.

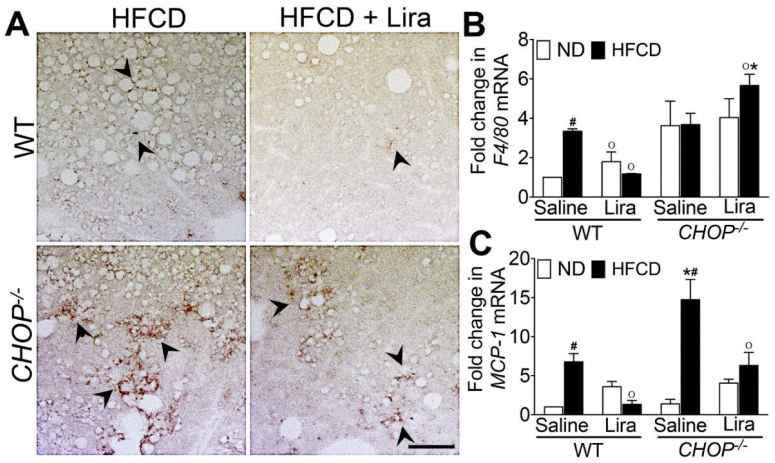

Figure 3. Hepatic macrophage infiltration is higher in HFCD-fed *CHOP*$^{-/-}$ mice

(A) Immunohistochemical staining of F4/80^{+} macrophages in the liver. Black arrows, F4/80^{+} macrophages. Quantitative RT-PCR analysis of (B) F4/80 and (C) MCP-1 mRNA transcript levels in the liver of WT or *CHOP*$^{-/-}$ mice fed a ND or HFCD for 16 weeks. After 12 weeks of feeding, mice received daily injections of saline or liraglutide (Lira) for 4 weeks. Data are presented as mean ± SEM; n = 5-7 mice per group. Hashtags indicate significant differences ($p < 0.05$) between ND- or HFCD-fed *CHOP*$^{-/-}$ mice. Stars indicate significant differences ($p < 0.05$) between WT and *CHOP*$^{-/-}$ mice. “o” indicate significant differences ($p < 0.05$) between saline or liraglutide treated *CHOP*$^{-/-}$ mice. Scale 20 μm.

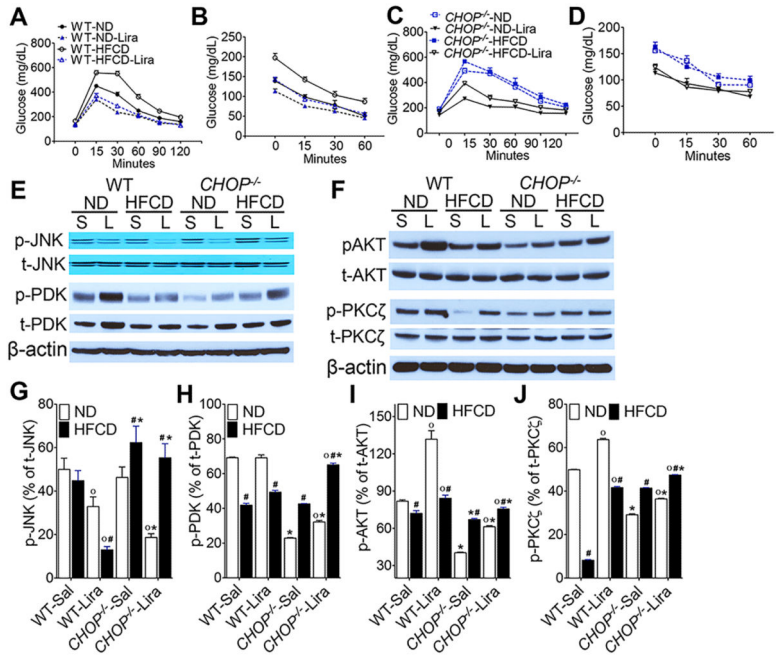

Figure 4. HFCD-fed *CHOP*$^{-/-}$ mice are resistant to liraglutide-mediated improvement in insulin sensitivity and glucose homeostasis

(A, C) Glucose and (B, D) insulin tolerance in (A, B) WT and (C, D) *CHOP*$^{-/-}$ mice fed a ND or HFCD for 16 weeks. After 12 weeks of feeding, mice received daily injections of saline (sal) or liraglutide (Lira) for 4 weeks. (E, F) Representative western blot images and (G-J) densitometry measurements of expression level of various effector molecules of the insulin-signaling pathway in the liver. Hashtags indicate significant differences ($p < 0.05$) between ND- or HFCD-fed mice. Stars indicate significant differences ($p < 0.05$) between WT and *CHOP*$^{-/-}$ mice. "o" indicate significant differences ($p < 0.05$) between saline or Liraglutide treated mice. Data are presented as mean ± SEM; n = 5-7 mice per group.

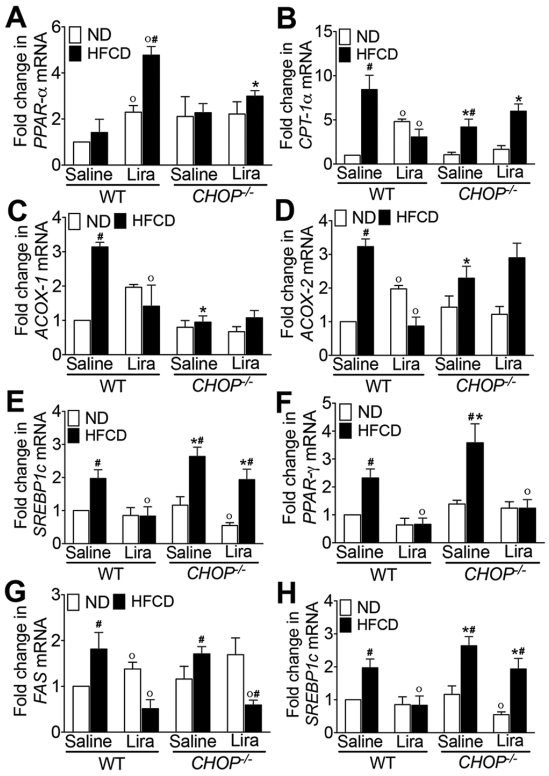

Figure 5. HFCD-fed *CHOP*$^{-/-}$ mice are resistant to liraglutide-mediated improvement in lipid, cholesterol and glucose metabolism

Quantitative RT-PCR analysis of (A) *PPAR-a*, (B) *CPT-1a*, (C) ACOX-1, (D) ACOX-2, (E) *SREBP1c*, (F) *PPAR-γ*, (G) FAS, and (H) ChREBP transcript levels in the liver of WT or *CHOP*$^{-/-}$ mice fed a ND or HFCD for 16 weeks. After 12 weeks of feeding, mice received daily injections of saline or liraglutide for 4 weeks. Data are presented as mean ± SEM; n = 5-7 mice per group. Hashtags indicate significant differences ($p < 0.05$) between ND- or HFCD-fed mice. Stars indicate significant differences ($p < 0.05$) between WT and *CHOP*$^{-/-}$ mice. “o” indicate significant differences ($p < 0.05$) between saline or Liraglutide treated mice.

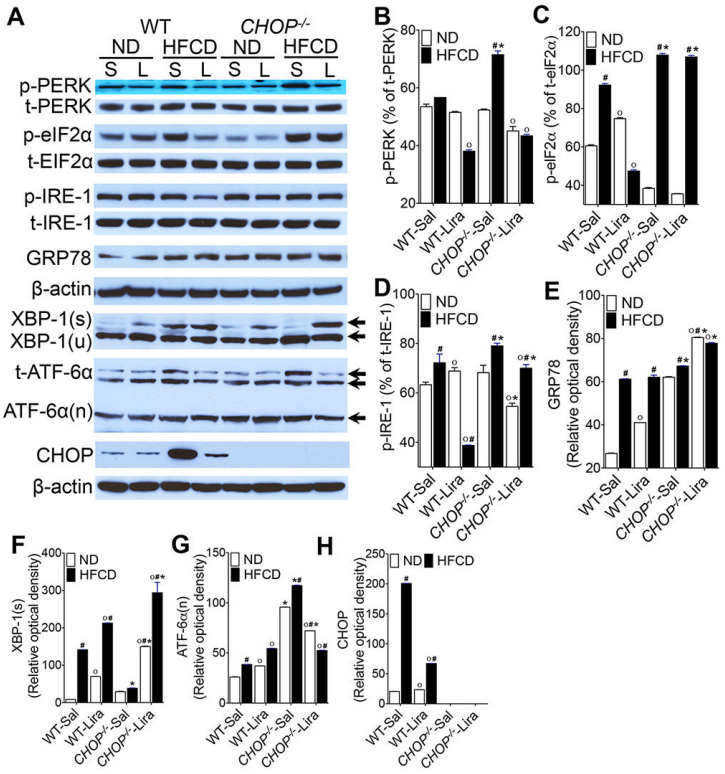

Figure 6. Liraglutide treatment attenuates ER stress in HFCD-fed WT mice but not in *CHOP*$^{-/-}$ mice

(A) Representative western blot images and (B-H) densitometry measurements of various ER stress parameters in the liver of WT and *CHOP*$^{-/-}$ mice fed a ND or HFCD for 16 weeks. After 12 weeks of feeding, mice received daily injections of saline (sal) or liraglutide (Lira) for 4 weeks. Data are presented as mean ± SEM; n = 5-7 mice per group. Hashtags indicate significant differences ($p < 0.05$) between ND- or HFCD-fed mice. Stars indicate significant differences ($p < 0.05$) between WT and *CHOP*$^{-/-}$ mice. “o” indicate significant differences ($p < 0.05$) between saline or Liraglutide treated mice.

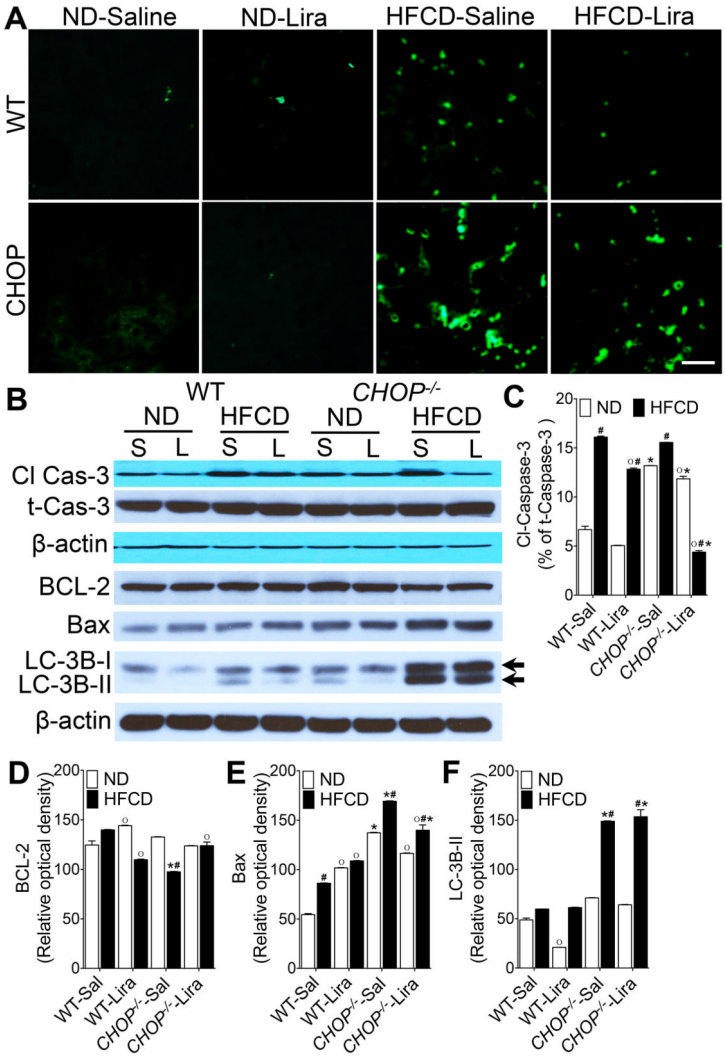

Figure 7. Liraglutide treatment suppresses apoptosis in HFCD-fed WT mice but not in *CHOP*$^{-/-}$ mice

(A) Representative immunofluorescence images of liver tissue sections stained with terminal deoxynucleotidyl transferase (TUNEL; green) to detect apoptotic cells. (B) Representative western blot images and (C-F) densitometry measurements of hepatic cleaved caspase 3, BCL-2, Bax and LC-3B expressions in WT and *CHOP*$^{-/-}$ mice fed a ND or HFCD for 16 weeks. After 12 weeks of feeding, mice received daily injections of saline (sal) or Liraglutide (Lira) for 4 weeks. Data are presented as mean ± SEM; n = 5-7 mice per group. Hashtags indicate significant differences ($p < 0.05$) between ND- or HFCD-fed mice. Stars indicate significant differences ($p < 0.05$) between WT and *CHOP*$^{-/-}$ mice. “o” indicate significant differences ($p < 0.05$) between saline or Liraglutide treated mice. Scale 20 μm.

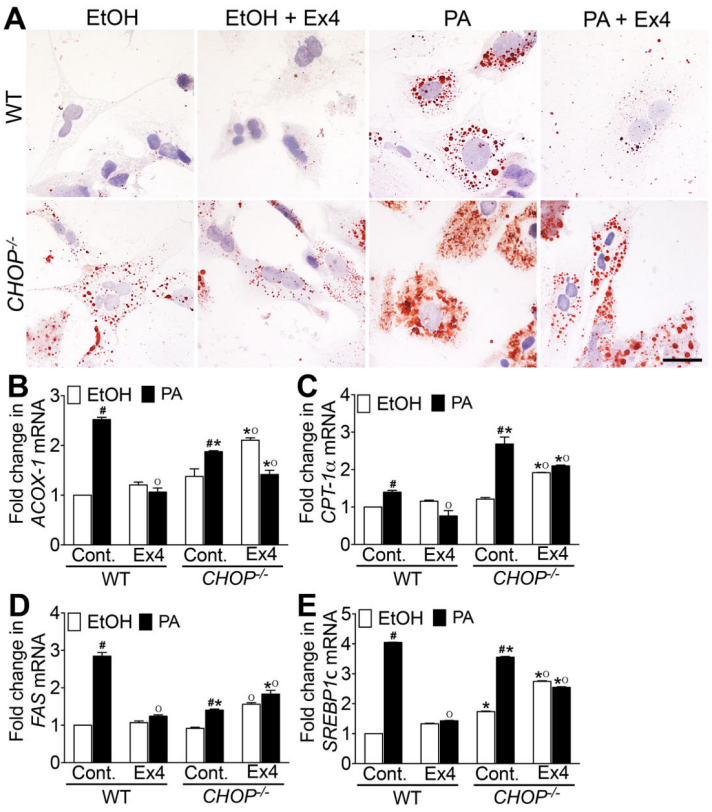

Figure 8. GLP-1 analog exendin-4 attenuates fatty acid deposition in primary hepatocytes from WT mice but not in primary hepatocytes from *CHOP*$^{-/-}$ mice

(A) Oil Red O stained micrographs of primary hepatocytes isolated from WT and *CHOP*$^{-/-}$ mice. Quantitative RT-PCR analysis of (B) ACOX-1, (C) CPT-1α, (D) FAS and (E) SREBP1c transcript levels in the primary hepatocytes isolated from WT and *CHOP*$^{-/-}$ mice. Hepatocytes were pretreated with 400 μM palmitic acid (PA) in ethanol for 24 h after which hepatocytes were treated with 10 nM exendin-4 and 400 μM PA for an additional 24 hr. Hepatocytes treated with ethanol (EtOH), or EtOH plus exendin-4 (Control + Ex4), or PA alone served as controls. Data presented are representative of 2 independent experiments with four replicates per treatment group. Hashtags indicate significant differences ($p < 0.05$) between EtOH or PA treated hepatocytes. Stars indicate significant differences ($p < 0.05$) between WT and *CHOP*$^{-/-}$ hepatocytes. "o" indicate significant differences ($p < 0.05$) between untreated or liraglutide treated mice. Scale 10 μm.